Self-assembled structures of hydrophobins HFBI and HFBII

Serimaa Ritva,[a]* Mika Torkkeli,[a] Arja Paananen,[b] Markus Linder,[b] Kaisa Kisko,[a] Matti Knaapila,[c] Olli Ikkala,[c] Elina Vuorimaa,[d] Helge Lemmetyinen[d] and Oliver Seeck[e]

[a]Department of Physical Sciences, P.O.B. 64, FIN-00014 University of Helsinki, Finland, [b]VTT Biotechnology, P.O.B. 1500, FIN-02044 VTT, Finland, [c]Department of Engineering Physics and Mathematics and Institute of New Materials, Helsinki University of Technology, P.O.B. 2200, FIN-02015 HUT, Espoo, Finland, [d]Department of Materials Chemistry, Tampere University of Technology, P.O.B. 541, FIN-33101 Tampere, Finland, [e]Forschungszentrum Juelich, IFF 8, D-52425 Juelich, Germany. E-mail: ritva.serimaa@Helsinki.fi

Hydrophobins are small proteins that function in the growth and development of fungi. The structures of class II hydrophobins HFBI and HFBII from Trichoderma reesei were studied using grazing incidence X-ray diffraction. HFBI was weakly ordered but HFBII formed a highly crystalline coating on water surface. Change from monoclinic to hexagonal structure was observed as the sample dried. The three-dimensional structures differed from the oblique two-dimensional structures observed in Langmuir-Blodgett monolayers of both HFBI and HFBII by atomic force microscopy.

Keywords: hydrophobin; grazing-incidence X-ray diffraction.

1. Introduction

Hydrophobins are fungal proteins, which have remarkable biophysical properties and diverse roles in fungal growth and development. They work as adhesive agents, as coatings, and lower the surface tension. They function also within the cell wall matrix affecting the wall composition (van Wetter *et al.*, 2000; Wösten 2001). In general the properties of hydrophobins seem to be related to their ability to self-assemble. Hydrophobins show large sequence variation within the group but always have four intrachain disulfide bridges in a special pattern (Fig. 1b). Depending on the hydrophobicity distribution of the primary sequence, hydrophobins can be divided into two classes, I and II. Class I hydrophobin SC3 is the most surface active protein known. Class I hydrophobins form highly insoluble coatings consisting of rodlets of 50–120 Å in diameter, which have shown to fulfill criteria for amyloid assemblies (de Vocth *et al.*, 2000; Mackay *et al.*, 2001). Class II hydrophobins form also assemblies at hydrophobic/hydrophilic interfaces, but dissociate in e.g. ethanol and sodium dodecyl sulfate (SDS). Amyloid-like rodlets have not been observed in coatings of class II hydrophobins (Wösten 2001).

The assemblages of class I hydrophobins have not been characterized by X-ray scattering even though there are several studies on amyloid rodlets (e.g. Blake *et al.*, 1996). Torkkeli *et al.* (2002) studied class II hydrophobins HFBI and HFBII from Trichoderma reesei (Nakari-Setälä *et al.*, 1997), by X-ray scattering and observed that samples of HFBI were amorphous but that those of HFBII were crystalline in the solid state. HFBII was observed to form needle-like crystals with diameters of 2-3 μm and lengths of 15-25 μm on an air bubble after mixing of the sample. In some cases needles up to several hundred μm were observed. HFBI also formed aggregates upon mixing but they were of less regular shape and more unstable than those of HFBII and dissolved during standing. In dilute aqueous solution both HFBI and HFBII existed mainly as monomers and dimers but in concentrated solutions they formed assemblages which have a radius of gyration of about 24 Å and a maximum dimension of about 65 Å, corresponding to a size of a tetramer (Torkkeli *et al.*, 2002). Monolayers of HFBI and HFBII were also made by Langmuir-Blogdett technique and according to atomic force microscopy (AFM) results both films were crystalline (Paananen *et al.*, 2002).

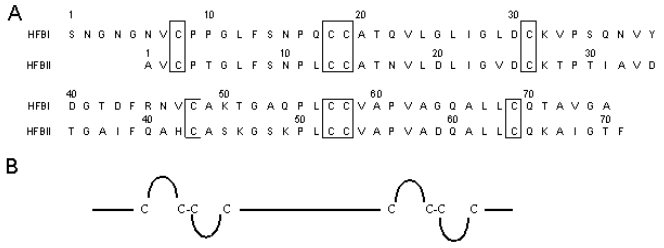

Figure 1
a) The primary sequences of HFBI and HFBII using the standard one-letter abbreviation for amino acids. b) The drawing shows how the Cys-residues form disulfides and the loops thus formed by the peptide chain. More detailed models of the structures of the proteins are not available. The sizes of the HFBI and HFBII monomers are 7.5 kDa and 7.2 kDa, respectively.

In this work spontaneously formed coatings of HFBI and HFBII at the air-water interface were studied by grazing incidence X-ray diffraction (GIXD). Grazing incidence diffraction is a powerful tool for structural studies of thin films and coatings and gives information on structures both parallel and perpendicular to the film surface (Als-Nielsen *et al.*, 1994). Two-dimensional structures of several protein monolayers at the air-water interface have been determined using synchrotron radiation (e.g. Weygand 1999; Verclas *et al.* 1999; Lenne *et al.*, 2000). Electron microscopy and atomic force microscopy give also information on the in-plane structure of protein monolayers (e.g. Avila-Sakar *et al.*, 1996; Czajkowski *et al.*, 1998; Reviakine *et al.*, 1998; Scheuring *et al.*, 1999). GIXD results are compared with results of AFM studies of HFBI and HFBII monolayers (Paananen *et al.*, 2002).

2. Experimental

2.1. Samples

HFBI was extracted from Trichoderma reesei strain VTT-D-98492 mycelium with 1% SDS in 0.2 M Na-acetate buffer pH 5.0. Buffer exchange to 15 mM Tris pH 9.0 buffer was then done by desalting on 10DG columns (BioRad, Hercules, CA). The sample was then loaded on a Resource Q column (Amersham Pharmacia Biotech, Uppsala, Sweden) and eluted with a linear salt gradient from 0 to 0.2 M NaCl. The HFBI peak fraction was then loaded onto a 1 $\times$ 20 cm Vydac C4 (Grace Vydac, Hesperia, CA) high performance liquid chromatography (HPLC) reversed phase column equilibrated with 0.1% TFA and eluted with a linear gradient of acetonitrile with 0.1% TFA. The HFBI peak fraction was finally lyophilized. HFBII was purified from the culture medium of a fermentation of Trichoderma reesei strain QM9414 by extraction with 2% of the non-ionic surfactant Berol 523 (Akzo-Nobel, Sweden). The extracted fraction was further purified by HPLC as described above and then lyophilized. Lyophilization was in all cases continued for 20 h at 0.2 mbar and a final temperature of 293 K.

Assemblages of hydrophobins are formed easily by shaking in most hydrophobin solutions. A concentration of 7.5 mg/ml hydrophobin was used in 0.1 M acetate buffer pH 5.0 with 20 mM $CuSO_4$ in a final volume of 0.9 ml. The solution was mixed on a laboratory shaker for one hour and then centrifuged using 5000 $\times g$ for 5 min. The pellet was then

characterized as such (Linder *et al.*, 2001). The primary sequences of HFBI and HFBII are shown in Fig. 1(a).

The Langmuir-Blodgett films were prepared with a KSV minitrough LB system (KSV Instruments). A 1 mM acetate buffer (pH = 5.0) in water purified by a Milli-Q system (Millipore) was used as a subphase. The temperature of the subphase was 18.0±0.5 °C. HFBI and HFBII were spread on the subphase from water solutions. After the surface pressure had stabilized for 20 min the monolayers were compressed at a rate of 10 mm/min to the deposition pressure of 30 mN/m. The films were transferred onto mica substrates by the vertical lifting method at a rate of 10 mm/min with transfer ratios near unity. AFM experiments are described in Paananen *et al.* (2002).

2.2. Grazing incidence X-ray diffraction experiments

GIXD experiments were performed at beamline W1.1 at Hamburger Synchrotronstrahlungslabor (HASYLAB) in Hamburg, Germany, with a wavelength of 1.24 Å. The beam was monochromatized by a double crystal Si(111) monochromator and focused on the sample, where its height and width were 1.5 and 4 mm, respectively. The beam was further reduced with slits to 0.1×1.5 mm. The scattering intensities were measured with a scintillation counter and the incident flux was monitored using an ionization chamber. The scans were performed both in the plane of the substrate surface (in-plane), which is horizontal, and in the plane containing the surface normal and the incident beam (out-of-plane). In both cases, the angle of incidence was held constant, 0.16°, during the scan and in the in-plane scans the vertical (take-off) angle was also 0.16°. The angular step was between 0.01 and 0.02° and receiving slits equivalent of 0.12 and 0.03° were used for in-plane and out-of-plane scans, respectively. The magnitudes of the scattering vector q were from 0.12 to 1.00 Å^{-1}, where $q = (4\pi/\lambda)\sin\theta$, 2θ is the scattering angle and λ the wavelength.

Hydrophobin was mixed in a drop of water on a silicon substrate. The in-plane and out-of-plane diffraction patterns were measured directly from the surface of the drop and from the deposited, dehydrated coating on the Si surface after dehydration. Note that in the former case the angle of incidence with respect to drop surface is not well defined. The measuring times were about 25 min/scan.

3. Results

The in-plane diffraction pattern of HFBI is shown in Fig. 2. Only one broad interference maximum is observed corresponding to Bragg distance of about 15.5 Å. The upturn of intensity towards $q = 0$ is mainly due to background scattering, which has not been subtracted.

HFBII was more ordered. On the droplet (Fig. 3) its structure is monoclinic, which has been determined earlier from an isotropic 'powder' sample (Torkkeli *et al.*, 2002) as being either space group 3 or 4 using a conventional X-ray source and a small angle X-ray scattering setup. The higher resolution of the synchrotron radiation based setup allows one to resolve more reflections and to confirm space group 4, $P112_1$, as the appropriate choice. The crystallites lie with their c-axis along the interface which is shown by the relative magnitude of the $hk0$ reflections and lack of $00l$ reflections in this scan (Fig. 3) which is made in the out-of-plane direction. The lattice constants are $a = 38.14$ Å, $b = 46.08$ Å, $c = 54.6$ Å and $\gamma = 122.3°$.

Subsequent scans were made from the dehydrated sample about 10 min later (Fig. 4). The out-of-plane scan now shows fewer and broader reflections indicating two dimensional hexagonal order with $a = b = 38.7$Å. The in-plane scan reveals additional reflections which show that the structure is three-dimensional hexagonal. The third axis, $c = 16.0$Å, is oriented parallel to the surface. The broadening of the reflections indicates that the size of the crystallites has diminished. The estimated size of the crystallites in the dry coating is roughly 600 Å which was determined from reflection 100 of the out-of-plane pattern using the Scherrer formula. The structure is essentially the same as in the lyophilized powder sample of the previous work (Torkkeli *et al.*, 2002), but the size of the crystallites is larger in the coating.

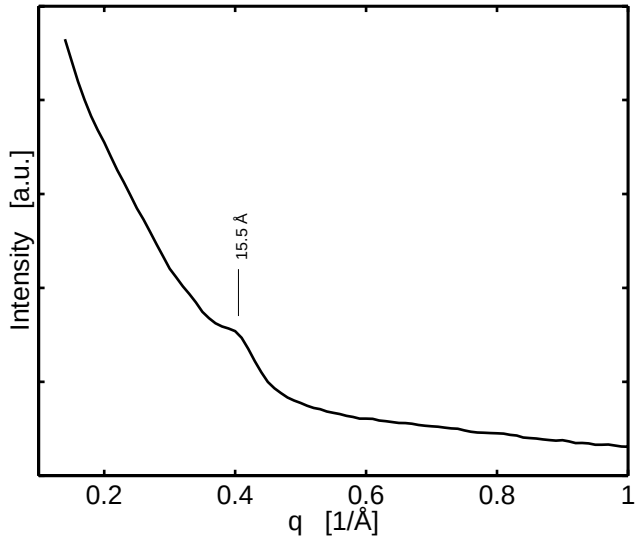

Figure 2
Scattering intensity of HFBI from the surface of a water droplet measured in the in-plane direction. The single reflection occurs at $q = 0.405$ Å^{-1}.

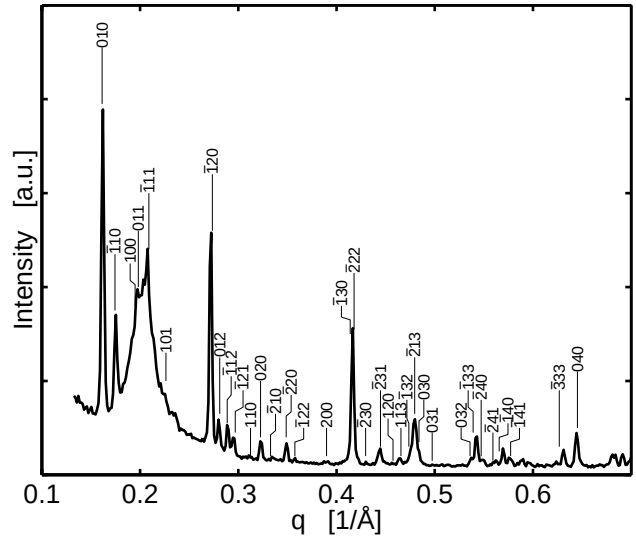

Figure 3
Scattering intensity of HFBII crystals on a water droplet measured in the out-of-plane direction. The indexation is based on monoclinic space group $P112_1$ using lattice constants $a = 38.14$ Å, $b = 46.08$ Å, $c = 54.6$ Å and $\gamma = 122.3°$

4. Discussion

The results of GIXD experiments show that especially HFBII spontaneously forms ordered layers at the air-water interface. HFBI was observed to form a weakly ordered coating on a water droplet. The only peak in the diffraction pattern (Fig. 2) might arise from a short range order of monomers. We cannot exclude that also HFBI crystallizes to

some extent, but its structure is unstable. Macromolecular crystals are held together by weak intermolecular interactions and can disintegrate in unfavorable conditions. In the previous X-ray scattering study on powder samples we were not able to detect long range order in HFBI samples. However, HFBI was observed to form unstable fibrillar assemblies in micrometer scale (Torkkeli *et al.*, 2002).

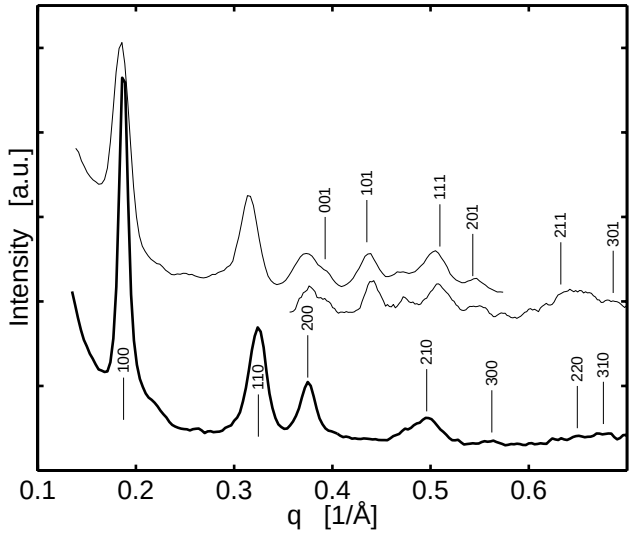

Figure 4
Scattering intensity of dehydrated HFBII on silicon surface. The indexation is according to hexagonal structure with $a = b = 38.7$ Å, $c = 16.0$ Å and $\gamma = 120^\circ$. The thick curve below is the intensity from the out-of-plane scan and the two upper curves are in-plane scans, lower of which is measured with better angular resolution using a receiving slit of 0.03°

HFBII was observed to be crystalline both on the droplet and as a dry coating (Fig. 2 and 3). The change from monoclinic to hexagonal form was observed as the sample dried. Previously it was observed that the crystal habit of HFBII is needlelike, which leads easily to preferred orientation of crystallites on the coating. The lattice constants could be determined more accurately in this work using synchrotron radiation. Polymorphism is not rare for protein crystals and may result from variation in crystallization conditions. In addition to humidity, temperature and pH may lead to different crystal forms for the same protein (e.g. Durbin & Feher 1996; Vilenchik *et al.*, 1998).

Little is known about the conformations and the shapes of the monomers. According to SAXS results of the previous study (Torkkeli *et al.* 2002) both HFBI and HFBII existed in concentrated solutions as tetramers, which were similar in size but different in shape. Low resolution shapes for HFBI (Paananen *et al.*, 2002) and HFBII (Torkkeli *et al.*, 2002) tetramers were resolved from solution SAXS data using the program Dammin (Svergun 1999). HFBI was torus-like and HFBII elongated with four branches. A similar tetramer conformation was observed to fit also to the SAXS intensity curve of the monoclinic powder sample at small values of q (Torkkeli *et al.*, 2002). We are trying to grow single hydrophobin crystals for a high resolution structure determination, but have not yet been succesful.

The easy formation of coatings is an unusual feature of hydrophobins. The difference in crystallinity of HFBI and HFBII may be related to their different roles in fungal development. HFBI is found in aggregated form in fungal cell wall and HFBII is found on spores (Nakari-Setälä *et al.*, 1997). According to Linder *et al.* (2000) some of their properties are different as well, e.g. HFBI has a higher affinity to surfactants and HFBII is more hydrophobic than HFBI.

AFM images of both HFBI and HFBII monolayers showed micropores of roughly 10–20 Å in diameter in a regular two-dimensional order. The depth of the pores could not be determined but the thickness of the layer is estimated roughly as 15 Å. This porous structure may be of importance from the point of view of applications. For example, Vilenchik *et al.*, (1998) have proposed that useful microporous materials can be obtained by using protein crystals, with a pore size range of 20 Å to more than 100 Å in diameter.

AFM data indicates an oblique structure for both HFBI and HFBII monolayers (Paananen *et al.*, 2002). The lattice constants of HFBI are $a = 59.2$Å, $b = 49.9$Å, $\gamma = 118.9^\circ$ and those of HFBII are $a = 58.7$Å, $b = 44.1$Å, $\gamma = 122.6^\circ$. The area of the unit cell of HFBI is slightly larger than that of HFBII, which may be due to different shapes and sizes of the deposited hydrophobins. In the two-dimensional lattices the angle γ is roughly 120°, which is close to the angle between the lattice vectors **a** and **b** in both three-dimensional lattices of HFBII, but lengths of lattice vectors a in the two-dimensional and three-dimensional unit cells differ notably.

It is interesting that HFBII has different structures as a monolayer and as a bulk coating and that HFBI was crystalline only as a monolayer. This may indicate that the protein conformations are not the same in bulk and monolayers. During the assembly of the monolayer onto surface the conformation of the monomers may change in such a way that hydrophilic and hydrophobic groups orient themselves at opposite sides on the coating. For Class I hydrophobin SC3 three different conformations have been revealed. One is observed in solution and two in the solid state. SC3 adopts α-helical state upon binding to a hydrophobic solid and β-sheet state, which is formed at the air-water interface (de Vocht *et al.*, 2002). The hydrophobin EAS was found to be largely unstructured in solution and to form amyloid-like structures (Mackay *et al.*, 2001).

5. Conclusions

HFBII was observed to form spontaneously a crystalline coating on a droplet and a change from monoclinic to hexagonal crystal form was verified as the sample dried. HFBI was weakly ordered on the air-water interface. However, both proteins have a tendency to self-organize on substrates, since crystalline monolayers could be produced from of them using Langmuir-Blodgett technique. It is known that interactions with the hydrophobic surface of the substrate and the buffer may affect the obtained two-dimensional structure (Lenne *et al.*, 2000). Thus interactions with the surface may stabilize the ordered structure of HFBI monolayer. The relation of the protein natural functions to the structures of the coatings is not yet known and deserves further studies. This study indicating different nanostructures for HFBI and HFBII is a step towards understanding of the assembly and functions of hydrophobins.

Financial support from the Academy of Finland is gratefully acknowledged.

References

Als-Nielsen, J., Jacquemain, D., Kjaer, K., Leveiller, F., Lahav, M. & Leiserowitz, L. (1994). *Phys. Rep.* **246**, 251-313.
Avila-Sakar, A.J. & Chiu, W. (1996). *Biophys. J.* **70**, 57-68.
Blake, C. & Serpell, L. (1996). *Structure* **4(8)**, 989-998.
Czajkowski, D.M., Sheng, S., & Shao, Z. (1998). *J. Mol. Biol.* **276**, 325-330.
Durbin, S.D. & Feher, G. (1996). *Annu. Rev. Phys. Chem.* **47**, 171-204.
Lenne, P-F., Bege, B., Renault, A., Zakri, C., Vénien-Bryan, C., Courty, S., Balavoine, F., Bergsma-Schutter, W., Brisson. A., Grübel. G., Boudet, N., Konoalov, O. & Legrand. J-F. (2000). *Biophys. J.* **79**, 496-500.
Linder, M., Selber, K., Nakari-Setälä, T., Qiao M., Kula, M-R., & Penttilä, M. (2000). *Biomacromolecules* **2**, 511-517.
Mackay, J.P., Matthews, J.M., Winefield, R.D., Mackay, L.G., Haverkamp, R.G., Templeton, M.D. (2001). *Structure* **9 (2)**, 83-91.

Nakari-Setälä, T., Aro, N., Ilmén, M., Muõz, G., Kalkkinen, N., & Penttilä, M. (1997). *Eur. J. Biochem.* **248**, 415-423.

Paananen, A., Vuorimaa, E., Linder, H. Lemmetyinen, M., Torkkeli, M., Serimaa, R., & Ikkala, O. (2002). Manuscript in preparation.

Reviakine, I., Bergsma-Schutter, W., & Brisson, A. (1998). *J. Struct. Biol.* **121**, 356-362.

Scheuring, S., Müller, D.J., Ringler, P., Heymann, J.B. & Engel, A. (1999). *J. of Microscopy* **193(1)** 28-35.

Svergun, D.I. (1999). *Biophys. J.* **76**, 2879-2886.

Torkkeli, M., Serimaa, R., Ikkala, O. & Linder, M. (2002). *Biophys. J.*, in press.

de Vocht, M. L. Reviakine I., Wösten H.A., Brisson A., Wessels J.G. & Robillard G.T. (2000). *J. Biol. Chem.* **275**, 28428-28432.

de Vocht, M., Reviakine, I., Ulrich, W.-P., Bergsma-Schutter, W., Wösten, H.A.B., Vogel, H., Brisson, A., Wessels, J.G.H., & Robillard G.T. (2002). *Protein Sci.* **11**, 1199-1205.

Verclas, S.A.W., Howes, P.B., Kjaer, K., Wurlitzer, A., Weygand, M., Büldt, G., Dencher, N.A., & Lösche, M. (1999). *J. Mol. Biol.* **287**, 837-843.

Vilenchik, L.Z., Griffith, J.P., St. Clair, N., Navia, M.A., & Margolin, A.L. (1998). *J. Am. Chem. Soc.* **120(18)**, 4290 -4294.

Wang, X., De Vocht, M.L., De Jonge, J., Poolman, B., Robillard, G.T. (2002). *Protein Science* **11(5)**, 1172-1181.

van Wetter, M.-A., Wösten, H.A.B., Sietsma, J.H. & Wessels J.G.H. (2000). *Fungal Genetics and Biology* **31**, 99-104.

Weygand,M., Wetzer, B., Pum, D., Sleytr, U.B., Cuvillier, N., Kjaer, K., Howes, P.B., & Lösche, M. (1999). *Biophys. J.* **76(1)**, 458-468.

Wösten, H. (2001). *Annu. Rev. Microbiol.* **55**, 625-646.

 Received 29 August 2002 • Accepted 3 January 2003